Tang, G., Barton, P., McNeill, L., Henstock, T., Tilmann, F., Dean, S., Jusuf, M., Djajadihardja, Y., Permana, H., Klingelhoefer, F., Kopp, H. (2013): 3-D active source tomography around Simeulue Island offshore Sumatra: thick crustal zone responsible for earthquake segment boundary. - Geophysical Research Letters, 40, 1, 48-53

DOI: 10.1029/2012GL054148

3-D active source tomography around Simeulue Island offshore Sumatra: Thick crustal zone responsible for earthquake segment boundary

Genyang Tang,[1,8] Penny J. Barton,[1] Lisa C. McNeill,[2] Timothy J. Henstock,[2] Frederik Tilmann,[1,3] Simon M. Dean,[2] Muhammad D. Jusuf,[4] Yusuf S. Djajadihardja,[4] Haryadi Permana,[5] Frauke Klingelhoefer,[6] and Heidrun Kopp[7]

Received 8 October 2012; revised 27 November 2012; accepted 29 November 2012; published 15 January 2013.

[1] We present a detailed 3-D *P*-wave velocity model obtained by first-arrival travel-time tomography with seismic refraction data in the segment boundary of the Sumatra subduction zone across Simeulue Island, and an image of the top of the subducted oceanic crust extracted from depth-migrated multi-channel seismic reflection profiles. We have picked *P*-wave first arrivals of the air-gun source seismic data recorded by local networks of ocean-bottom seismometers, and inverted the travel-times for a 3-D velocity model of the subduction zone. This velocity model shows an anomalous zone of intermediate velocities between those of oceanic crust and mantle that is associated with raised topography on the top of the oceanic crust. We interpret this feature as a thickened crustal zone in the subducting plate with compositional and topographic variations, providing a primary control on the upper plate structure and on the segmentation of the 2004 and 2005 earthquake ruptures. **Citation:** Tang, G., P. J. Barton, L. C. McNeill, T. J. Henstock, F. Tilmann, S. M. Dean, M. D. Jusuf, Y. S. Djajadihardja, H. Permana, F. Klingelhoefer, and H. Kopp (2013), 3-D active source tomography around Simeulue Island offshore Sumatra: Thick crustal zone responsible for earthquake segment boundary, *Geophys. Res. Lett.*, *40*, 48–53, doi:10.1029/2012GL054148.

1. Introduction

[2] Large megathrust earthquakes occurring at subduction zones generally only rupture a segment of the plate boundary fault in each event. Along-strike propagation of such ruptures may be obstructed by geometric discontinuities in the subducted plate such as slab tears [e.g., *Cummins et al*., 2002], topographic anomalies on the subducting plate such as seamount chains, ridges and fracture zones [e.g., *Robinson et al*., 2006], or major upper plate structures [e.g., *Melnick et al*., 2006]. Subduction of large-scale seamounts, ridges, or even fracture zones has been proposed to increase local seismic coupling in subduction zones [e.g., *Scholz and Small*, 1997; *Robinson et al*., 2006] or, contrastingly, reduce coupling [e.g., *Mochizuki et al*., 2008; *Wang and Bilek*, 2011]. Increased interplate coupling may generate rupture barriers, as proposed for the Southwest Japan [*Kodaira et al*., 2000], Costa Rican [*Bilek et al*., 2003], and South American subduction zones [*Robinson et al*., 2006]. In other regions where, conversely, decreased coupling is suggested, basal erosion and faulting within the overriding plate, and/or sediment migration and fluid interaction may cause stress heterogeneity on the megathrust fault [*Wang and Bilek*, 2011; *Mochizuki et al*., 2008], forming a weak zone and thus inhibiting accumulation of elastic strain, also acting as a barrier to rupture.

[3] The Sumatra subduction zone also shows distinct segments of megathrust rupture, particularly the 2004 and 2005 ruptures [e.g., *Ammon et al*., 2005; *Briggs et al*., 2006], with segment boundaries demarcated by changes in coseismic slip and aftershock distribution [e.g., *Briggs et al*., 2006; *Chlieh et al*., 2007; *Tilmann et al*., 2010]. The segment boundary between the 2004 $M_w = 9.2$ Aceh-Andaman earthquake and the 2005 $M_w = 8.7$ Nias earthquake is identified at central Simeulue Island, where there seems to be a narrow and persistent barrier [*Briggs et al*., 2006; *Meltzner et al*., 2012]. *Franke et al*. [2008], among others, proposed that this barrier is controlled by a reactivated fossil fracture zone (96° FZ on Figures 1 and 2) associated with the Wharton Fossil Ridge (Figure 1), which may have developed into a ramp or a shallow slab tear beneath the forearc. To investigate the structure of the 2004–2005 segment boundary of the Sumatra subduction zone, we provide a detailed, well-resolved 3-D velocity model of the region with an image of the top surface of the subducting plate and oceanic crustal thickness relative to seismicity distribution. This study improves our understanding of the influence of subducting oceanic crustal structure on rupture behavior and provides insight into the primary controls on the segmentation of megathrust earthquakes in subduction zones.

2. Data and Methods

[4] 3-D refraction data were collected around Simeulue Island in 2008 using ocean-bottom seismometers (OBS) [*Minshull et al*., 2005] and an air-gun source of total capacity

---

All Supporting Information may be found in the online version of this article.

[1]Bullard Laboratories, University of Cambridge, Cambridge, UK.
[2]National Oceanography Centre Southampton, University of Southampton, Southampton, UK.
[3]GFZ German Research Centre for Geosciences, Helmholtz Centre Potsdam, Telegrafenberg, Potsdam, Germany.
[4]Agency for the Assessment and Application of Technology (BPPT), Jakarta, Indonesia.
[5]Indonesian Institute of Sciences (LIPI), Bandung, Indonesia.
[6]IFREMER, Plouzané, France.
[7]GEOMAR Helmholtz-Centre for Ocean Sciences Kiel, Kiel, Germany.
[8]State Key Laboratory of Petroleum Resource and Prospecting, China University of Petroleum, Beijing, China.

Corresponding author: G. Tang, China University of Petroleum, Beijing, China. (phoenixfree@gmail.com)

0094-8276-/13/2012GL054148

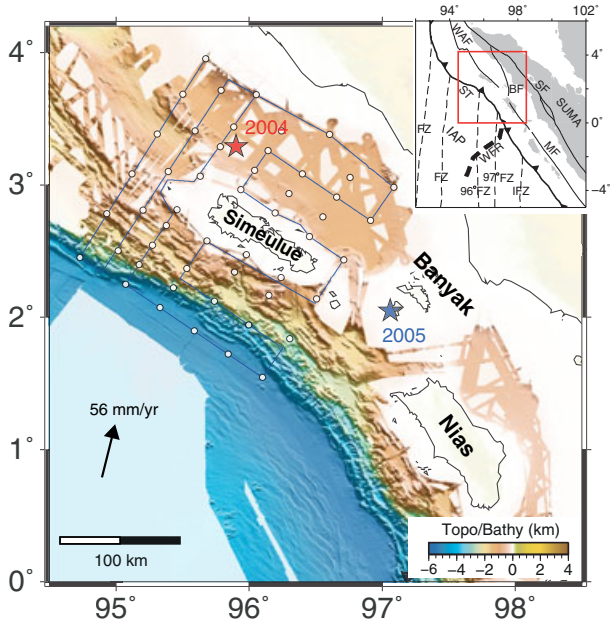

Figure 1. Geometry of the 3-D seismic refraction survey showing OBS sites (white circles) and air-gun profiles (blue lines). Swath bathymetry are from our and previous surveys [*Henstock et al*., 2006; *Graindorge et al*., 2008; *Ladage et al*., 2006]. Black arrow shows the plate motion of the Indo-Australian plate relative to the Eurasia plate based on *Prawirodirdjo and Bock* [2004]. (inset) Tectonic setting and major faults based on *Berglar et al*. [2010]. Red box: study area; Thick dashed lines: Wharton Fossil Ridge (WFR); thin dashed lines: interpreted fossil fracture zones. IAP = Indo-Australian Plate, SUMA = Sumatra, SF = Sumatran Fault, WAF = West-Andaman Fault, BF = Batee Fault, MF = Mentawai Fault, ST = Sumatra Trench, FZ = Fracture Zone, IFZ = Investigator Fracture Zone.

5420 cubic inch (Figure 1). Fifty OBSs were deployed in an area 203 km × 192 km, and 10,462 air-gun shots were fired along 1550 km of profiles. About 125,000 *P*-wave first-arrival refractions were picked from the OBS data and inverted to give a velocity model. First-arrival travel-time data from two additional 2-D OBS refraction surveys approximately coincident with the northwest and southeast boundaries of the 3-D refraction survey area were also included in the velocity inversion [*Klingelhoefer et al*., 2010]. The tomography method is that of *Zelt and Barton* [1998], which inverts the travel-times picked from these local active-source experiments for the velocity model. The Supporting Information describes details of the tomography as well as resolution tests. The horizontal resolution is 10–20 km in the top 15 km of the model, except immediately under Simeulue. At depths larger than ~20 km, horizontal resolution is 20–40 km, and only the structures less than ~100 km from the trench are resolved (i.e., underneath and seaward of Simeulue). The vertical resolution is about 5 km. The velocity model inverted from the first-arrival travel-time tomography was later used to relocate local earthquake events from October 2005 to March 2006 recorded by a passive seismic network installed in approximately the same area [*Tilmann et al*., 2010] (Figures 2 and 3) using a tomographic inversion technique [*Eberhart-Phillips*, 1990]. The velocity model is allowed to be simultaneously updated with the earthquake locations. From this data set, relocations were made for events with hypocenter depth 8–50 km, with more than 10 records of each event, and initial travel-time residual < 0.5 s.

[5] Multichannel seismic data (MCS) were also acquired in the area, and processed with the conventional Kirchhoff prestack depth migration method. The top of oceanic crust (TOC) of the subducting plate was picked and interpolated from the depth-migrated MCS profiles seaward of Simeulue (see Supporting Information). TOC picks from other depth-migrated MCS profiles digitized from *Franke et al*. [2008] were also included in the interpolation and smoothing (see auxiliary material). The integrated TOC surface is assumed to represent the plate interface in the subduction zone (Figure 2).

3. Results

[6] Trench-normal and trench-parallel sections extracted from the 3-D velocity model are shown in Figure 3. Shallow sediments with velocities lower than 4 km/s are confined to a thin surface layer (1–6 km in thickness) in both the accretionary prism and the forearc basin. The deep part of the

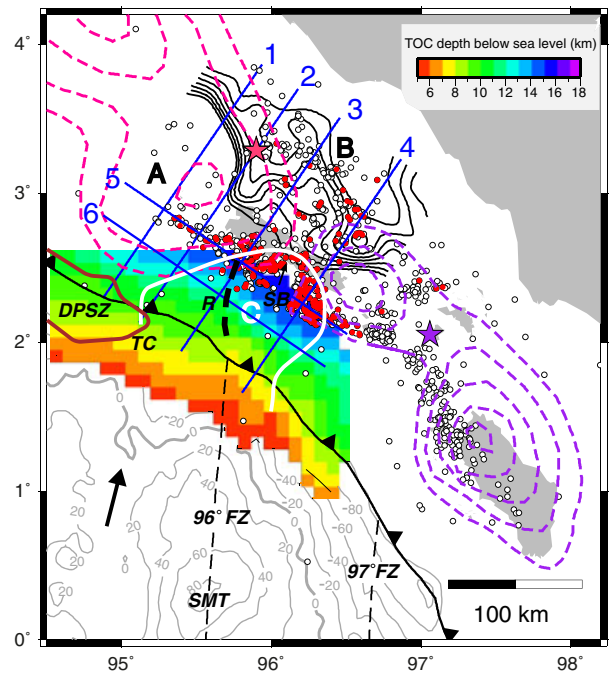

Figure 2. Geophysical setting of the segment boundary region around Simeulue Island. The top surface of the TOC picked from depth-migrated MCS data is plotted in color. Free-air gravity is shown by gray contours [*Sandwell and Smith*, 2009]. Coseismic slip of the 2004 (pink) and 2005 (purple) earthquakes is shown by dashed contours at 5 and 2 m intervals, respectively [*Chlieh et al*., 2007; *Briggs et al*., 2006]. Red (well-resolved) and white circles: seismicity relocated with the 3-D velocity model (see text); Thick black contours: outlines of the backstop from the 6 km/s velocity contours at 1 km intervals; White curved line: outline of the TCZ (see text); Blue lines: velocity cross-sections shown in Figure 3. A = Accretionary wedge, B = Backstop, C = Thickened oceanic crust, TC = Trench trend change, FZ = fracture zone, SMT = seamount, DPSZ = different property sediment zone [*Dean et al*., 2010].

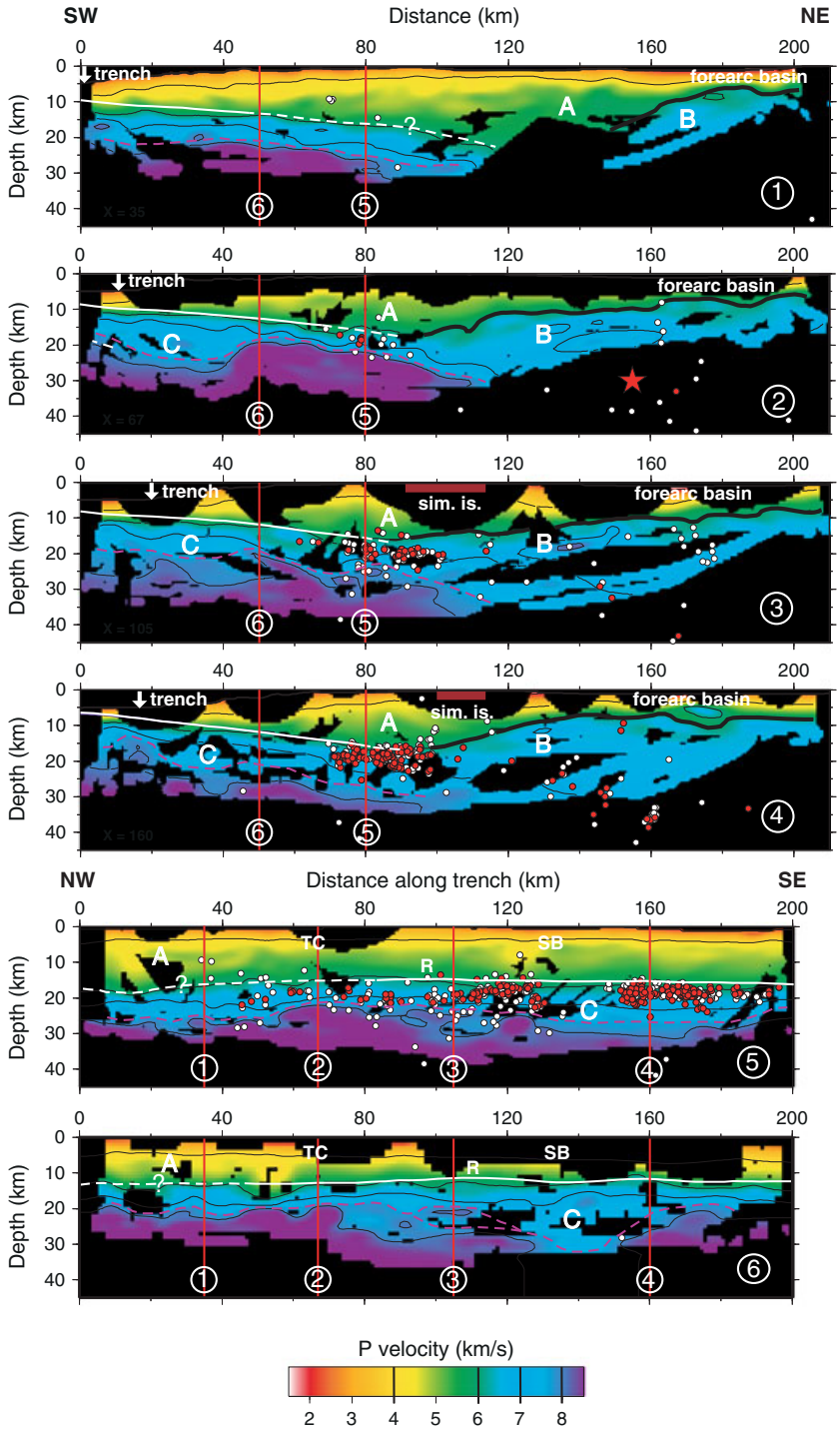

Figure 3. Velocity cross-sections extracted from the velocity model inverted from the first-arrival travel-time tomography (contoured at 4, 6, 7, and 8 km/s). Relocated earthquake locations are plotted within ±10 km of Line 1–4 and ±5 km of Line 5–6. Thick black lines: top of the backstop; Solid white lines: the TOC constrained by the MCS data; Dashed white lines: unconstrained TOC; Dashed purple lines: possible oceanic Moho interface approximated by the 7.6 km/s velocity contours; Thin red lines: intersection location of velocity cross-sections; 'sim. is.' = Simeulue Island, SB = segment boundary. Other symbols and labels same as in Figure 2.

accretionary wedge (marked A in Figures 2 and 3) with velocities of 4–5.5 km/s, extends from the Sumatra trench to the forearc high (Figures 1 and 2). The active accretionary wedge is much wider and thicker to the NW of the 2004 epicenter area than to the SE (the transition occurring between lines 1 and 2 in Figure 2) [*Dean et al.*, 2010; *Henstock et al.*, 2006]. The variation in the width and thickness of the accretionary wedge along strike is coincident with a change in the trend of the deformation front (marked TC in Figure 2), suggesting a shift in the geometric setting of the subduction zone.

[7] The higher velocity material (6–8 km/s) beneath the accretionary wedge is interpreted as the oceanic plate in

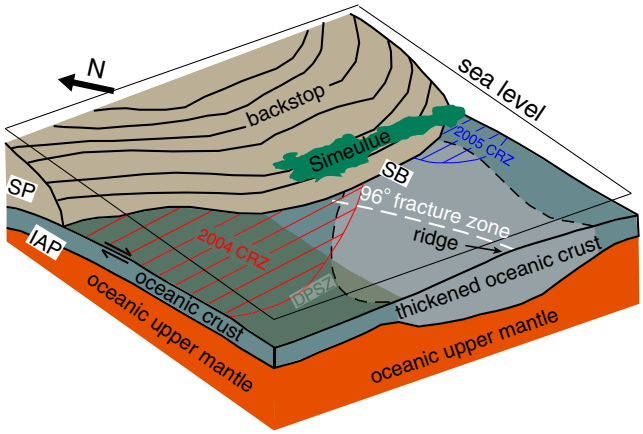

Figure 4. Cartoon illustrating the segmentation of the 2004–2005 megathrust rupture in the Sumatra subduction zone around Simeulue Island. The accretionary complex removed for simplicity. CRZ: coseismic rupture zone; SP: Sunda plate. Other labels same as in Figures 2 and 3.

the region seaward of Simeulue Island and as the upper plate 'backstop' block (older forearc material) landward of the island. This 'backstop' block, outlined by the 6 km/s contour surface (marked B in Figures 2 and 3), is located beneath the forearc basin, slopes seaward and bulges seaward at Simeulue Island. It is likely to act as a mechanical boundary in the subduction zone.

[8] Another striking feature identified in the velocity model is a broad zone of anomalous velocities (7.2–7.7 km/s) below 15–20 km depth from sea level along the normal-to-trench direction seaward of Simeulue Island (marked C in Figures 2 and 3), in contrast to higher velocities (>8 km/s) along strike to the NW and SE. Zero velocity variations relative to the averaged along-strike velocities at fixed depths from the TOC define the boundary of this anomalous crustal zone (see auxiliary Figure S12), which is about 100 km wide along strike at the trench and extends for at least 100 km perpendicular to the trench (Figure 2), and shows a velocity range intermediate between oceanic crust and mantle. These velocities could indicate either partially serpentinized oceanic mantle or thicker oceanic crust. We prefer the latter interpretation because the observed raised topography of the TOC is consistent with underplating of oceanic crustal material to the base of the crust. The TOC under the accretionary prism shows a broad topographic high seaward of Simeulue (marked R in Figure 2). Near the trench, this topographic high has an amplitude up to 3 km over a distance of ~90 km both to the NW and SE, and appears to extend seaward onto the oceanic plate, evident from a series of gravity and bathymetric highs (Figures 1 and 2), which are usually interpreted as fracture zone structures (Figure 1, inset). We note that bathymetric and gravity data indicate these interpreted fracture zones have variable surface expression along their extent (Figures 1 and 2), possibly suggesting a more complex origin.

[9] The distribution of local earthquakes [*Tilmann et al*., 2010], relocated using the 3-D velocity model inverted from the first-arrival travel-time data, shows a concentration along and below the top surface of the subducting plate. Few earthquakes occur in the accretionary prism (Figures 2 and 3), suggesting that recent deformation within the prism is minimal or aseismic. Another pronounced feature of the seismicity is a landward indentation of the main belt of earthquake epicenters at central Simeulue [e.g., *Tilmann et al*., 2010].

4. Discussion and Conclusion

[10] The anomalous oceanic crustal zone we interpret as thickened crust is generally thicker than the crust both to the NW and to the SE (see Figure 4). The thickness is greatest offshore central Simeulue and perhaps beneath the island. Along line 6 the Moho surface is estimated to lie at ~25–30 km depth in the thickened crustal zone (TCZ), and the TOC high lies at ~11 km depth (Figures 2 and 3), implying a thickness of ~14–19 km. To the SE of the TCZ, the oceanic crust thins to ~7–8 km (Figure 3, Lines 5, 6). To the NW of the TCZ and the change in strike of the deformation front (TC in Figure 2), the crust thickness appears to be variable, between 5 and 10 km (Figure 2 and Figure 3, Lines 1, 2, 5, 6). There appears to be a small patch of ~10 km thick crust here (see auxiliary Figure S12 and Figure 3, Line 1) whose size is at the limit of the resolution scale. However, 2-D crustal modeling in this region [*Klingelhoefer et al*., 2010] and further to the NW [*Singh et al*., 2011] shows thinner crust (~5 km), suggesting that this may be a localized feature. Interestingly, the seaward-dipping upper plate backstop, bulging seaward at Simeulue Island, is coincident with the subduction of the TCZ and the segment boundary on the megathrust. This observation may suggest a correlation between the seaward-dipping backstop and anomalous coupling at the segment boundary, similar to observations in the central Cascadia subduction zone [e.g., *Tréhu et al*., 2012].

[11] The topographic low in coseismic uplift estimated from geodetic and paleo-seismological data from central Simeulue has been used to argue in favor of reduced interplate coupling here [*Briggs et al*., 2006; *Meltzner et al*., 2012]. *Briggs et al*. [2006] can constrain this segment boundary to be less than 70 km wide along strike from local uplift data, which is comparable to the 100 km wide thickened crust. *Franke et al*. [2008] proposed that a tear or a ramp associated with the inferred 96° fracture zone may create this segment boundary. We observe a ramp with a vertical offset ~1 km over an along-strike distance of ~25 km to the east of the TOC high immediately offshore Simeulue, which might be associated with the inferred fracture zone. However, such a small offset of the fracture zone is unlikely to act as a topographic barrier to great rupture during an event such as the 2004 M_w 9.2 earthquake. Fracture zones of similar width and offset on the oceanic basement are also imaged to the NW of this inferred fracture zone [*Singh et al*., 2011]; however, those fracture zones did not stop the 2004 rupture. Therefore, the existence of the segment boundary may require an integrated interpretation beyond structural/topographic control.

[12] We emphasize the significance of the change of physical properties on the megathrust associated with sediment lithology and fluid distribution, which may be driven by the contrast in oceanic crustal properties, and their subsequent impact on rupture segmentation. *Dean et al*. [2010] propose that the TOC high may act as a barrier to sediment transport along the trench generating contrasting properties of input sediment and seismic properties of the developing megathrust fault on either side of the barrier, which must have existed for several million years as the TCZ has been

subducting beneath the accretionary prism over a down-trench distance of at least 100 km. The megathrust section with distinct seismic properties NW of the barrier is marked as DPSZ on Figures 2 and 4. The overlying sediments, probably derived from different lithology, are suggested to be denser and mechanically stronger than those to the SE [*Dean et al*., 2010] due to dewatering and lithification during burial [*Gulick et al*., 2011], contributing to strengthening of the megathrust. We speculate that the TCZ itself might be intrinsically compositionally weak relative to adjacent regions indicated by the velocity variations, which could potentially change the rheology of the megathrust in the segment boundary. The TCZ structure and topography may further intensify the contrast in the megathrust strength. The inferred fracture zone, a preexisting structure coincident with the TCZ, could be a locus of enhanced fluid release into the megathrust [*Tilmann et al*., 2010]. Such a localized influence could explain the indentation of the seismicity band (stable sliding/seismogenic zone transition), suggesting an along-strike change in physical properties on the megathrust. This physical property change at the TCZ may in turn influence the frictional behavior on the megathrust, leading to weak interplate coupling and aseismic slip [e.g., *Moore and Saffer*, 2001].

[13] We propose that the TCZ, with associated compositional (indicated by seismic velocity) and topographic changes, provides a primary control on the segmentation of subduction zone rupture along the Sumatra megathrust through impact on sediment and megathrust properties (Figure 4). The possible intrinsically weak nature of this anomalous crustal section, and/or physical property changes across it, may additionally result in heterogeneous frictional behavior and specifically reduced interplate coupling at the segment boundary, thus creating a clearly persistent and distinct earthquake segment boundary.

[14] **Acknowledgments.** We thank the master and crew of the F/S *Sonne* and all those involved in SO198 cruises for their assistance, and our partners BPPT, Jakarta, and LIPI, Bandung for their logistical assistance. The OBSs were provided by the UK Ocean Bottom Instrumentation Facility. This work was funded by Natural Environment Research Council (NE/D004381/1). We thank the Dorothy Hodgkin Postgraduate Award for funding a PhD studentship and the CUP Science Foundation for financial support (No. YJRC-2013-33). We thank Satish Singh for useful discussion and ideas, and referees Anne Tréhu and Nathan Bangs for their suggestions for improving this paper.

References

Ammon, C. J., C. Ji, H. Thio, D. Robinson, S. Ni, V. Hjorleifsdottir, H. Kanamori, T. Lay, S. Das, D. Helmberger, G. Ichinose, J. Polet, and D. Wald (2005), Rupture process of the 2004 Sumatra-Andaman earthquake, *Science*, *308*(5725), 1133-1139, doi:10.1126/science.1112260.

Berglar, K., C. Gaedicke, D. Franke, S. Ladage, F. Klingelhoefer, and Y. Djajadihardja (2010), Structural evolution and strike-slip tectonics off north-western Sumatra, *Tectonophysics*, *480*, 119-132, doi:10.1016/j.tecto.2009.10.003.

Bilek, S. L., S. Y. Schwartz, and H. R. DeShon (2003), Control of seafloor roughness on earthquake rupture behavior, *Geology*, *31*(5), 455-458, doi:10.1130/0091-7613(2003)031<0455:COSROE>2.0.CO;2.

Briggs, R. W., K. Sieh, A. J. Meltzner, D. Natawidjaja, J. Galetzka, B. Suwargadi, Y. Hsu, M. Simons, N. Hananto, I. Suprihanto, D. Prayudi, J. Avouac, L. Prawirodirdjo, and Y. Bock (2006), Deformation and slip along the Sunda megathrust in the great 2005 Nias-Simeulue earthquake, *Science*, *311*(5769), 1897-1901, doi:10.1126/science.1122602.

Chlieh, M., J. Avouac, V. Hjorleifsdottir, T. A. Song, C. Ji, K. Sieh, A. Sladen, H. Hebert, L. Prawirodirdjo, Y. Bock, and J. Galetzka (2007), Coseismic slip and afterslip of the great Mw 9.15 Sumatra-Andaman earthquake of 2004, *Bulletin of the Seismological Society of America*, *97*(1A), S152-S173, doi:10.1785/0120050631.

Cummins, P. R., T. Baba, S. Kodaira, and Y. Kaneda (2002), The 1946 Nankai earthquake and segmentation of the Nankai Trough, *Physics of Earth Planet Interior*, *132*, 75-87, doi:10.1016/S0031-9201(02)00045-6.

Dean, S. M., L. C. McNeill, T. J. Henstock, J. M. Bull, S. P. S. Gulick, J. A. Austin, N. L. B. Bangs, Y. S. Djajadihardja, and H. Permana (2010), Contrasting décollement and prism properties over the Sumatra 2004-2005 earthquake rupture boundary, *Science*, *329*, 207-210, doi:10.1126/science.1189373.

Eberhart-Phillips, D. (1990), Three-dimensional P and S velocity structure in the Coalinga Region, California, *Journal of Geophysical Research*, *95*(B10), 15,343-15,363, doi:10.1029/JB095iB10p15343.

Franke, D., M. Schnabel, S. Ladage, D. R. Tappin, S. Neben, Y. S. Djajadihardja, C. Muller, H. Kopp, and C. Gaedicke (2008), The great Sumatra-Andaman earthquakes- imaging the boundary between the ruptures of the great 2004 and 2005 earthquakes, *Earth and Planetary Science Letters*, *269*, 118-130, doi:10.1016/j.epsl.2008.01.047.

Graindorge, D., et al. (2008), Impact of lower plate structure on upper plate deformation at the NW Sumatran convergent margin from seafloor morphology, *Earth and Planetary Science Letters*, *275*(3-4), 201-210, doi:10.1016/j.epsl.2008.04.053.

Gulick, S. P. S., J. A. Austin, L. C. McNeill, N. L. B. Bangs, K. M. Martin, T. J. Henstock, J. M. Bull, S. Dean, Y. D. Djajadihardja, and H. Permana (2011), Updip rupture of the 2004 Sumatra earthquake extended by thick indurated sediments, *Nature Geoscience*, *4*, 453-456, doi:10.1038/ngeo1176.

Henstock, T. J., L. C. McNeill, and D. R. Tappin (2006), Seafloor morphology of the Sumatran subduction zone: Surface rupture during megathrust earthquakes? *Geology*, *34*(6), 485-488, doi:10.1130/22426.1.

Klingelhoefer, F., M.-A. Gutscher, S. Ladage, J.-X. Dessa, D. Graindorge, D. Franke, C. André, H. Permana, T. Yudistira, and A. Chauhan (2010), Limits of the seismogenic zone in the epicentral region of the 26 December 2004 great Sumatra-Andaman earthquake: Results from seismic refraction and wide-angle reflection surveys and thermal modeling, *J. Geophy. Res.*, *115*, B01304, doi:10.1029/2009JB006569.

Kodaira, S., N. Takahashi, A. Nakanishi, S. Miura, and Y. Kaneda (2000), Subducted seamount imaged in the rupture zone of the 1946 Nankaido earthquake, *Science*, *289*(5476), 104-106, doi:10.1126/science.289.5476.104.

Ladage, S., C. Gaedicke, U. Barckhausen, I. Heyde, W. Weinrebe, E. R. Flueh, A. Krabbenhoeft, H. Kopp, S. Fajar, and Y. Djajadihardja (2006), Bathymetric survey images structure off Sumatra, *Eos Transactions, American Geophysical Union*, *87*(17), 165, doi:10.1029/2006EO170001.

Melnick, D., B. Bookhagen, H. P. Echtler, and M. P. Strecker, 2006, Coastal deformation and great subduction earthquakes, Isla Santa María, Chile (37º S), *Geological Society of America Bulletin*, *118*, 1463-1480, doi:10.1130/B25865.1.

Meltzner, A. J., K. Sieh, H. Chiang, C. Shen, B. W. Suwargadi, D. H. Natawidjaja, B. Philibosian, and R. W. Briggs (2012), Persistent termini of 2004- and 2005-like ruptures of the Sunda megathrust, *J. Geophys. Res.*, *117*, B04405, doi:10.1029/2011JB008888.

Minshull, T. A., M. C. Sinha, and C. Peirce (2005), Multidisciplinary subseabed geophysical imaging, *Sea Technology*, *46*(10), 27-31.

Mochizuki, K., T. Yamada, M. Shinohara, Y. Yamanaka, and T. Kanazawa (2008), Weak interplate coupling by seamounts and repeating M 7 earthquakes, *Science*, *321*, 1194-1197, doi:10.1126/science.1160250.

Moore, J. C., and D. Saffer (2001), Updip limit of the seismogenic zone beneath the accretionary prism of southwest Japan: An effect of diagenetic to low grade metamorphic processes and increasing effective stress, *Geology*, *29*(2), 183-186, doi:10.1130/0091-7613(2001)029<0183:ULOTSZ>2.0.CO;2.

Prawirodirdjo, L. and Y. Bock (2004), Instantaneous global plate motion model from 12 years of continuous GPS observations, *Journal of Geophysical Research*, *109*, B08405, doi:10.1029/2003JB002944.

Robinson, D. P., S. Das, and A. B. Watts (2006), Earthquake rupture stalled by subducting fracture zone, *Science*, *312*, 1203-1205, doi:10.1126/science.1125771.

Sandwell, D. T., and W. H. F. Smith (2009), Global marine gravity from retracked Geosat and ERS-1 altimetry: Ridge segmentation versus spreading rate, *J. Geophys. Res.*, *114*, B01411, doi:10.1029/2008JB006008.

Scholz C. H., and C. Small (1997), The effect of seamount subduction on seismic coupling, *Geology*, *25*, 487-490, doi:10.1130/0091-7613(1997)025<0487:TEOSSO>2.3.CO;2.

Singh, S. C., H. Carton, A. S. Chauhan, S. Androvandi, A. Davaille, J. Dyment, M. Cannat, and N. D. Hananto (2011), Extremely thin crust in the Indian Ocean possibly resulting from Plume-Ridge interaction, *Geophys. J. Int.*, *184*(1), 29-42, doi:10.1111/j.1365-246X.2010.04823.x.

Tilmann, F., T. J. Craig, I. Grevemeyer, B. Suwargadi, H. Kopp, and E. Flueh (2010), The updip seismic/aseismic transition of the Sumatra megathrust illuminated by aftershocks of the 2004 Aceh-Andaman and 2005 Nias

events, *Geophys. J. Int.*, *181*(3), 1261-1274, doi:10.1111/j.1365-246X.2010.04597.x.

Tréhu, A. M., R. J. Blakely, and C. W. Mark (2012), Subducted seamounts and recent earthquakes beneath the central Cascadia forearc, *Geology*, *40*(2), 103-106, doi:10.1130/G32460.1.

Wang, K., and S. L. Bilek (2011), Do subducting seamounts generate or stop large earthquakes? *Geology*, *39*(9), 819-822, doi:10.1130/G31856.1.

Zelt, C. A., and P. J. Barton (1998), Three-dimensional seismic refraction tomography: A comparison of two methods applied to data from the Faeroe Basin, *Geophys. J. Int.*, *103*(B4), 7187-7210, doi:10.1029/97JB03536.